

# Effects of thermal boundary condition on turbulent statistics in flows with a supercritical fluid

**Hassan Nemati, Ashish Patel, Bendiks Jan Boersma, Rene Pecnik**

Process and Energy Department, Delft University of Technology,  
Leeghwaterstraat 39, 2628 CB Delft, The Netherlands



# Motivation

Several numerical studies on heat transfer to supercritical fluids

- Effect of buoyancy, heat flux/mass flux ratio, etc.
- Yoo, Annual Review Fluid Mechanics, 2013

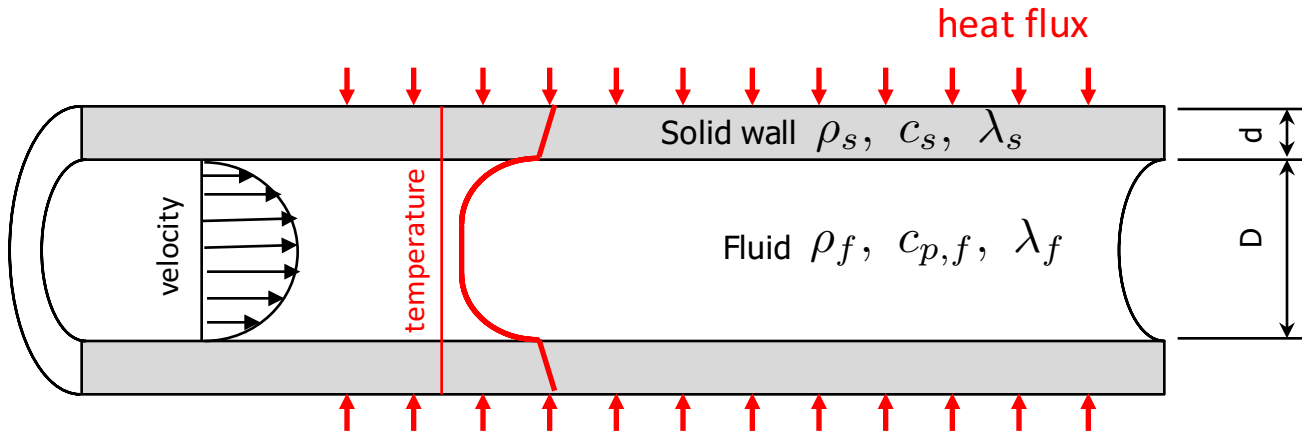
Most of the numerical studies assume isoflux boundary conditions

- Isoflux BC allows temperature fluctuations at the wall
- Isothermal BC does not allow temperature to fluctuate at the wall

If fluid's Prandtl number  $> 1$ , temperature fluctuations do not affect heat transfer (Kasagi, 1989; Li et al., 2009).

**Does this also hold for flows with strong property gradients even if  $\text{Pr} > 1$ ?**

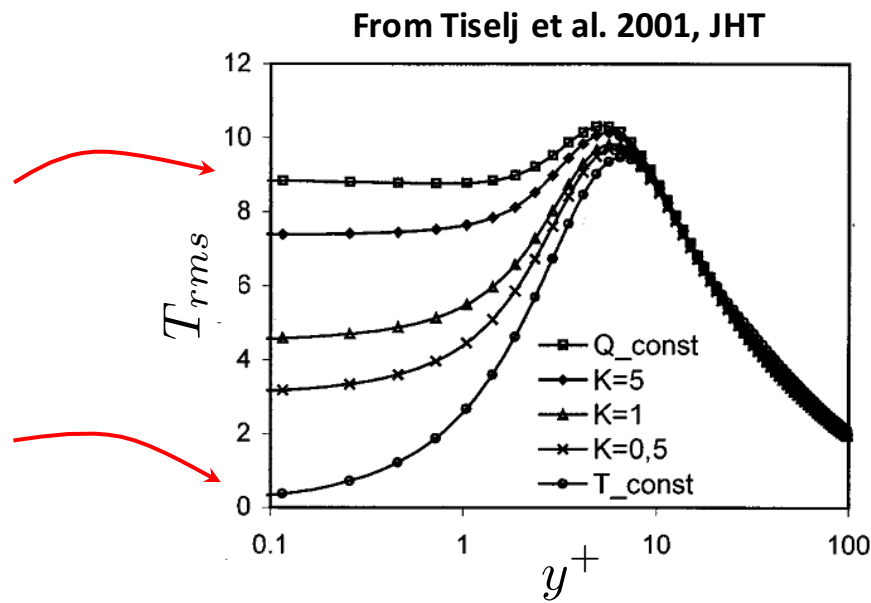
# Effect of fluid/wall properties on temperature fluctuations



Thermal effusivity ratio:

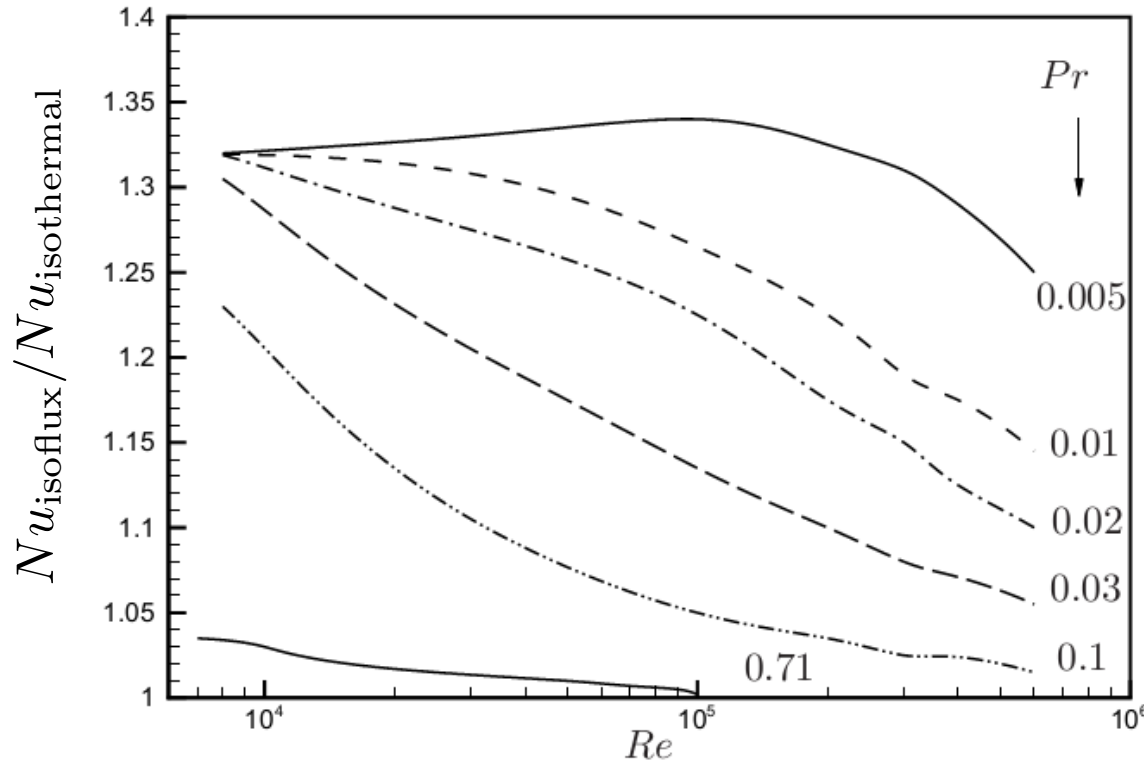
$$K = \sqrt{\frac{\rho_f c_{p,f} \lambda_f}{\rho_s c_s \lambda_s}} \rightarrow \infty : \text{isoflux BC}$$

$$K = \sqrt{\frac{\rho_f c_{p,f} \lambda_f}{\rho_s c_s \lambda_s}} \rightarrow 0 : \text{isothermal BC}$$



# Effect of Prandtl number

- Ratio of Nusselt number for isoflux to isothermal boundary conditions



Sleicher, 1955; Kasagi et al., 1989

# Thermal effusivity ratio and Prandtl number examples

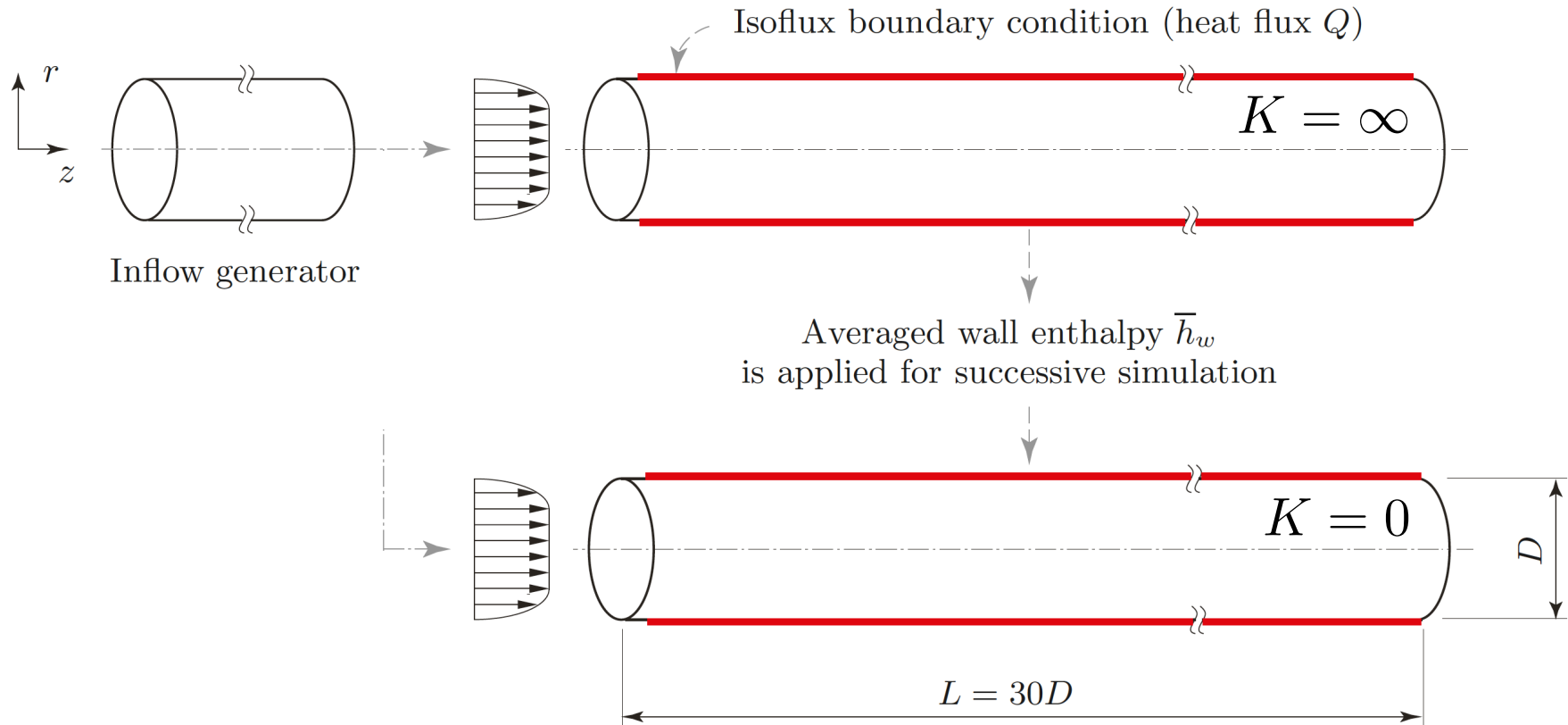
Prandtl number	Air * 0.708	Water * 6.78	scCO <sub>2</sub> (80bar) up to 14
Aluminum	0.00025	0.071	
Nickel based alloy	0.00073	0.207	~0.25
Copper	0.00015	0.044	
Glass	0.00419	1.190	
Plexiglas	0.00942	2.680	

\* based on Kasagi et al., Journal of heat transfer, 1989

Investigate influence of thermal effusivity ratio on heat transfer to scCO<sub>2</sub>

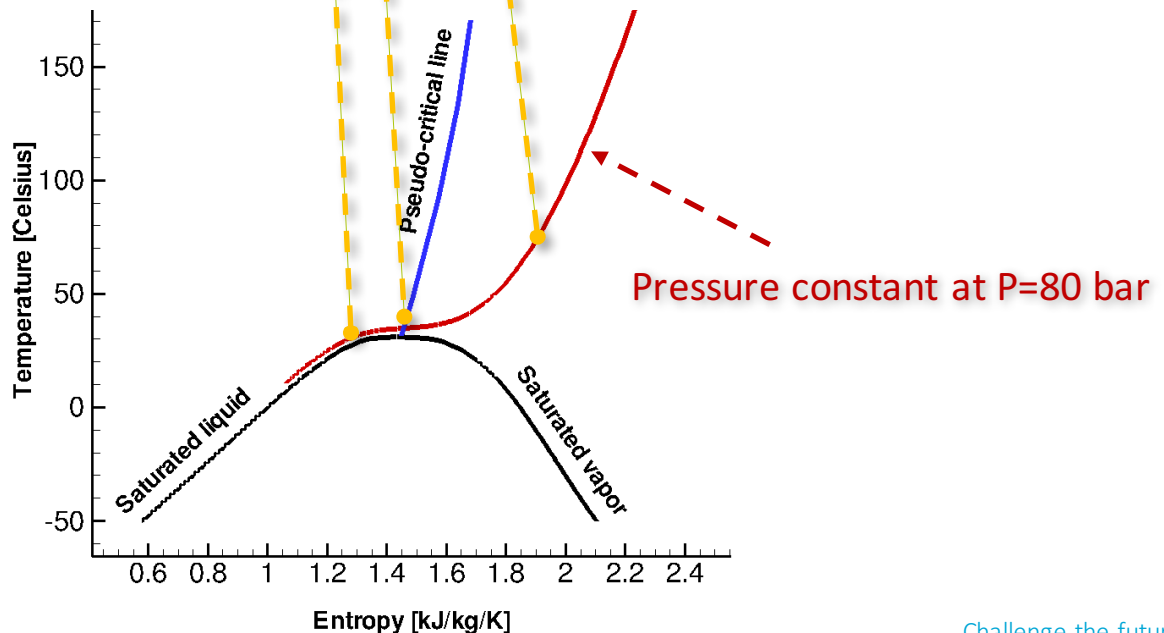
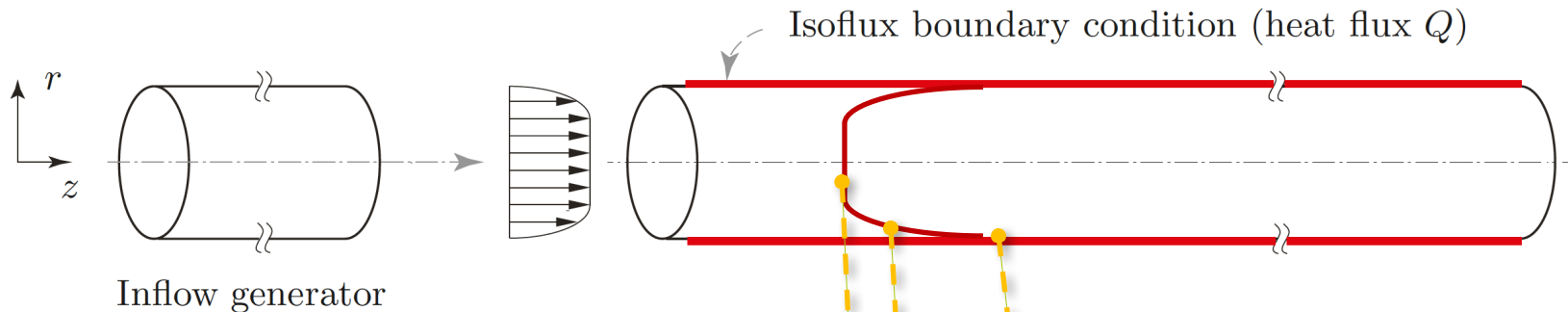
- Allow wall temperature fluctuations:  $K = \infty$
- Do not allow temperature fluctuations:  $K = 0$

# Simulation setup

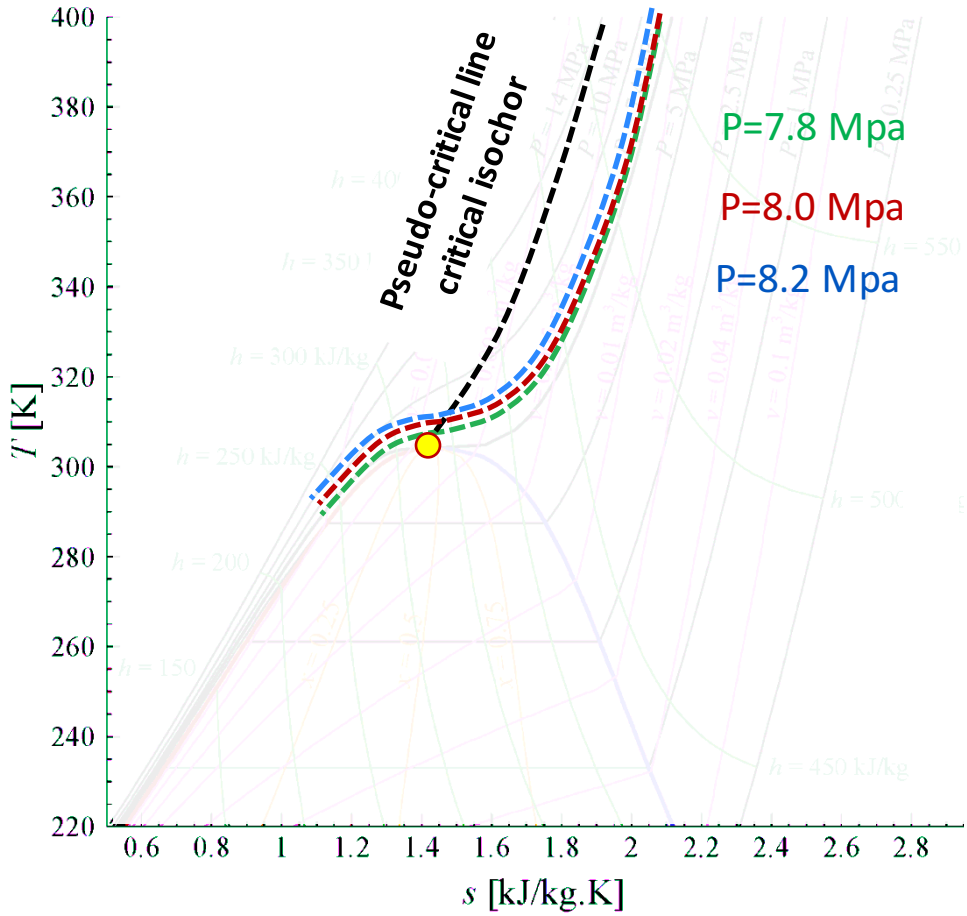


This setup ensures the same thermodynamic condition at the wall!

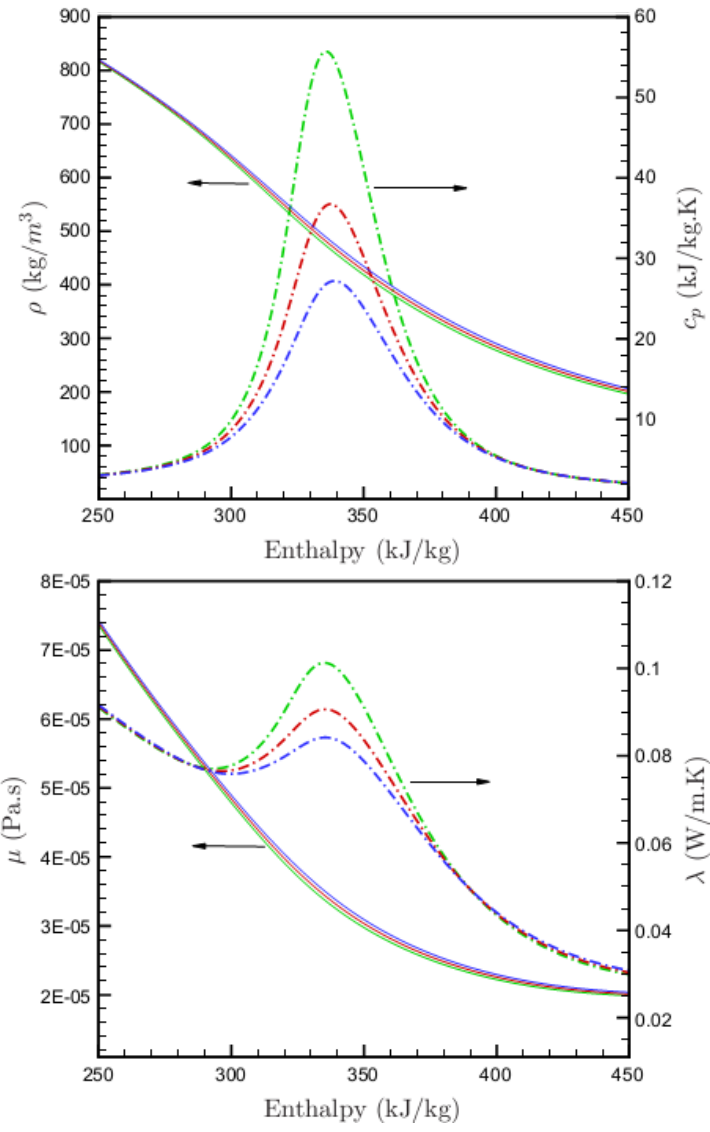
# Simulation setup



# Properties of supercritical fluids



T-s Diagram including the critical point for  $\text{CO}_2$



# Governing equations

Low-Mach number approximation of Navier-Stokes equations:

$$\frac{\partial \rho}{\partial t} + \frac{\partial \rho u_i}{\partial x_i} = 0$$

$$\frac{\partial \rho u_i}{\partial t} + \frac{\partial \rho u_i u_j}{\partial x_j} = -\frac{\partial p}{\partial x_i} + \frac{1}{Re_{\tau 0}} \frac{\partial \tau_{ij}}{\partial x_j}$$

$$\frac{\partial \rho h}{\partial t} + \frac{\partial \rho u_i h}{\partial x_i} = -\frac{1}{Re_{\tau 0} Pr_0} \frac{\partial q_i}{\partial x_i}$$

$$\tau_{ij} = \mu S_{ij} = \mu \left( \frac{\partial u_i}{\partial x_j} + \frac{\partial u_j}{\partial x_i} - \frac{2}{3} \frac{\partial u_k}{\partial x_k} \delta_{ij} \right)$$

$$q_i = -\lambda \frac{\partial T}{\partial x_i} = -\frac{\lambda}{c_p} \frac{\partial h}{\partial x_i} = -\alpha \frac{\partial h}{\partial x_i}$$

with:

$$Re_{\tau 0} = \frac{\rho_0^* u_{\tau 0}^* D^*}{\mu_0^*} = 360$$

$$Pr_0 = \frac{\mu_0^* c_{p0}^*}{\lambda_0^*} = 3.2$$

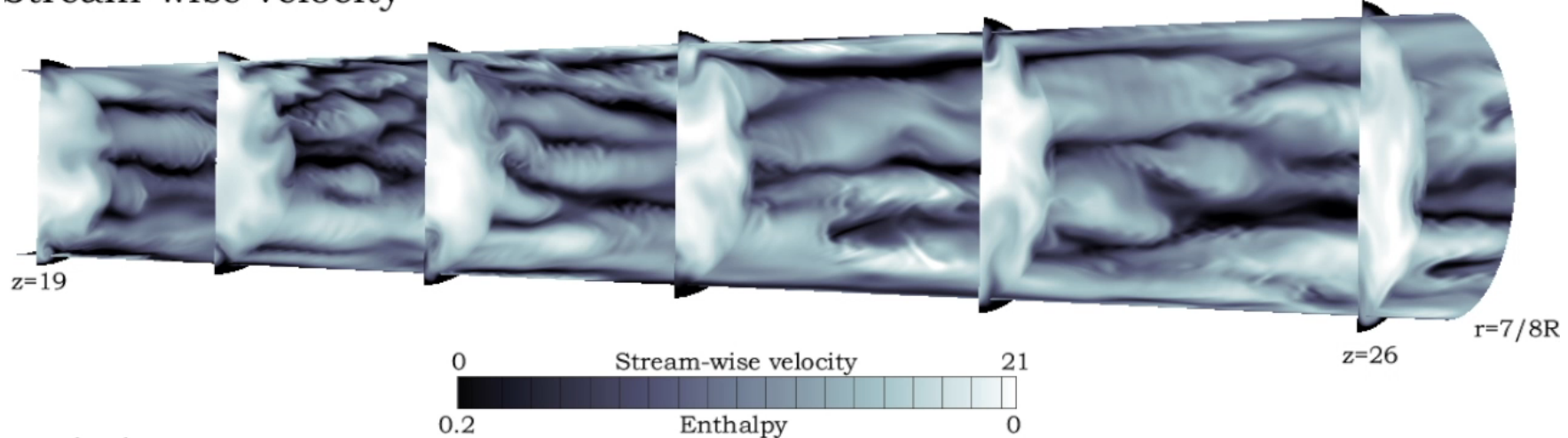
$$Q = \frac{q_w^* D^*}{\lambda_0^* T_0^*} = Re_{\tau 0} Pr q = 2.4$$

# Numerical scheme

- **Spatial discretization:** 2<sup>nd</sup> order central difference on staggered mesh
- **Temporal discretization:** 2<sup>nd</sup> Adams-Bashforth and Adams-Moulton
- Koren limiter for advection part of energy equation
- Diffusion part in circumferential direction treated implicitly
- Mesh resolution:
  - Mesh points 128 x 288 x 1728
  - Radial  $0.55 \text{ (wall)} < \Delta r^+ < 4.3 \text{ (center)}$
  - Circumferential  $R\Delta\theta^+ = 3.93$
  - Axial  $\Delta z^+ = 6.25$
- **Thermophysical properties (CO<sub>2</sub> at P=8 Mpa)** are interpolated from table

# Instantaneous flow field, isoflux simulation

Stream-wise velocity

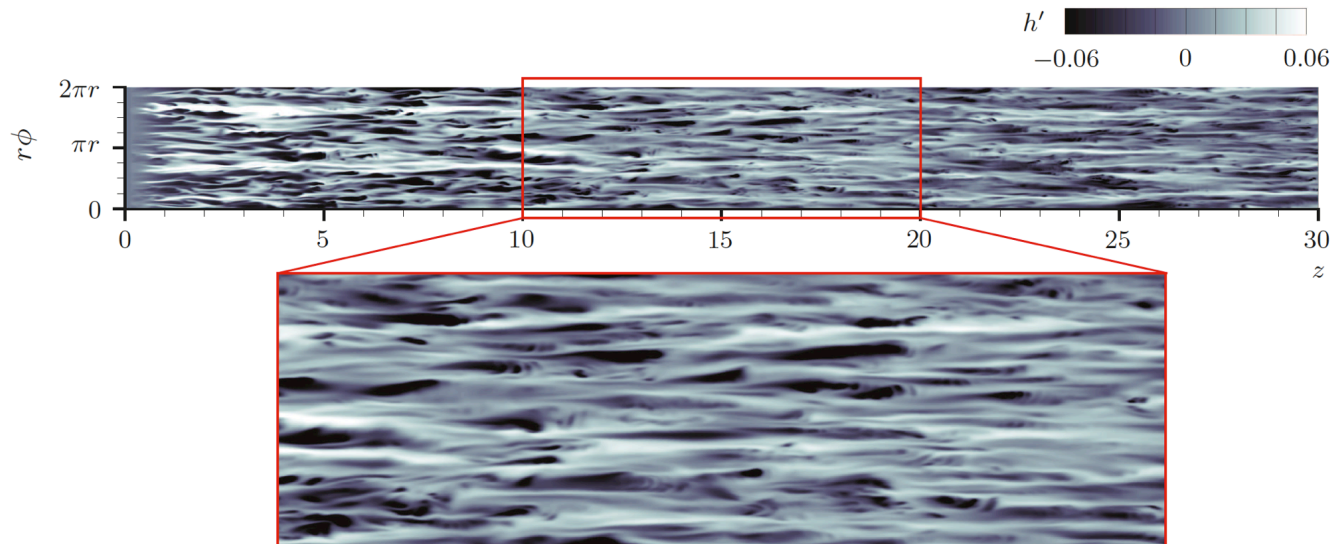


Enthalpy

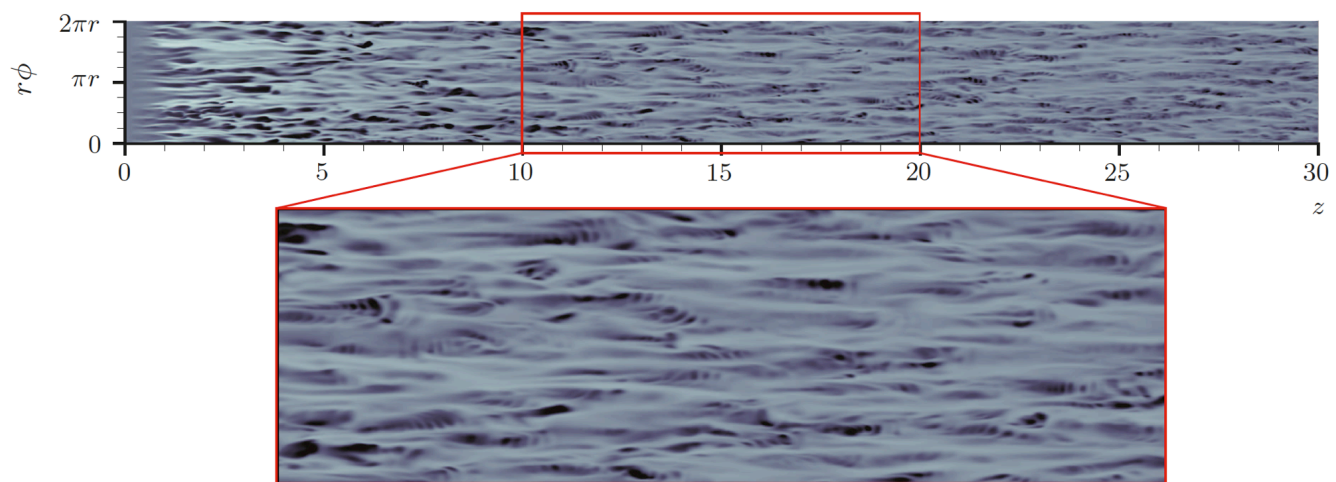


# Instantaneous enthalpy fluctuations

Iso-flux

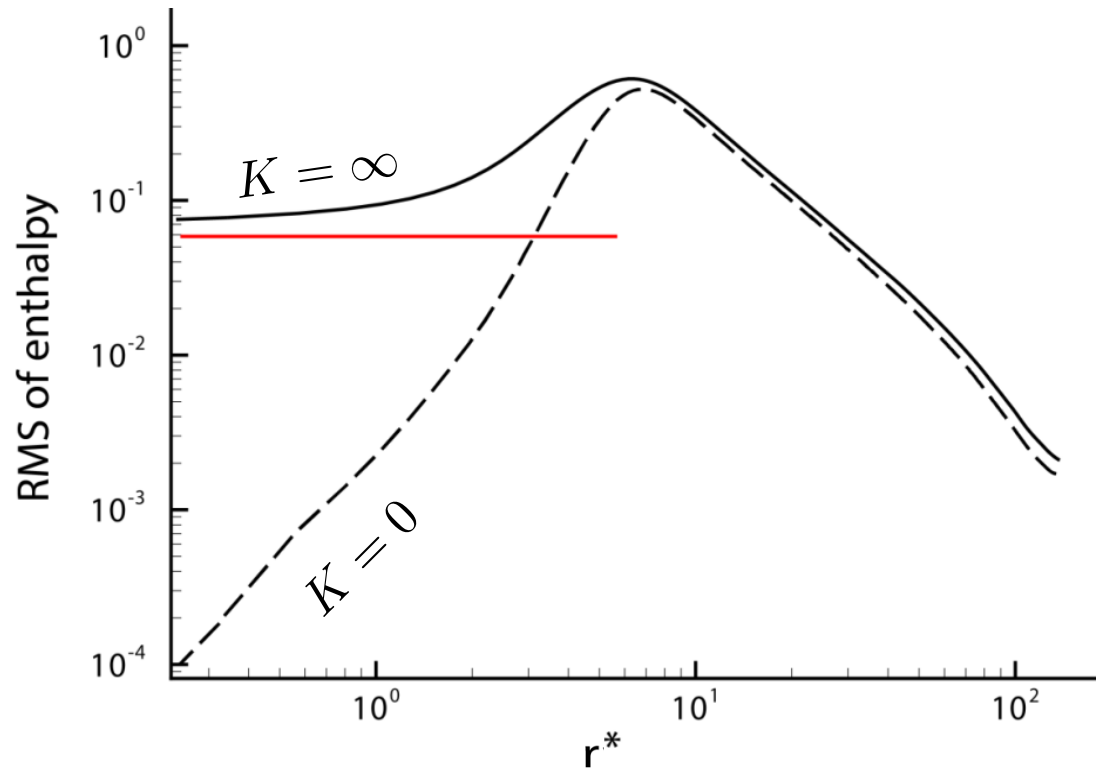
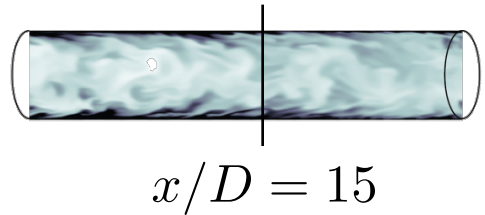


Iso-thermal



$$y^+ = 4.7 \text{ (based on inlet condition)}$$

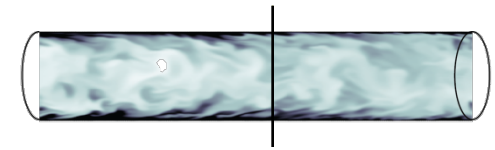
# Enthalpy rms profiles



# Radial heat fluxes

Total radial heat flux:

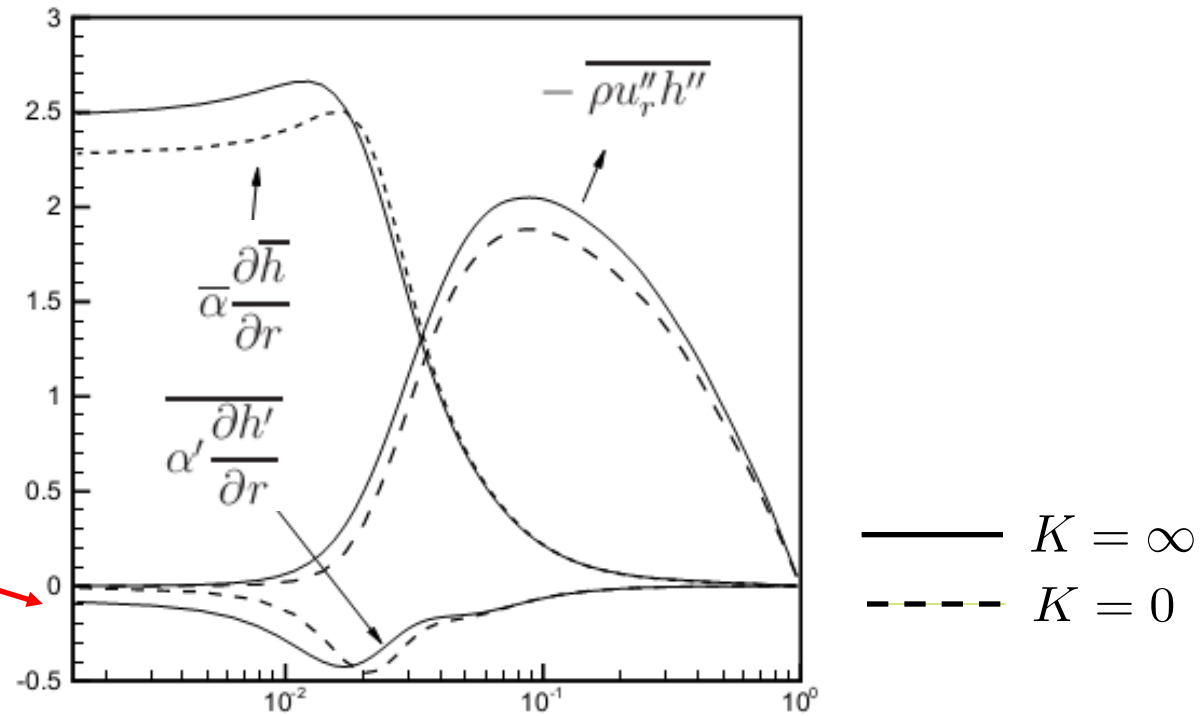
$$q_{r,tot} = \bar{\alpha} \frac{\partial \bar{h}}{\partial r} + \alpha' \frac{\partial h'}{\partial r} - \overline{\rho u_r'' h''}$$



$$x/D = 15$$

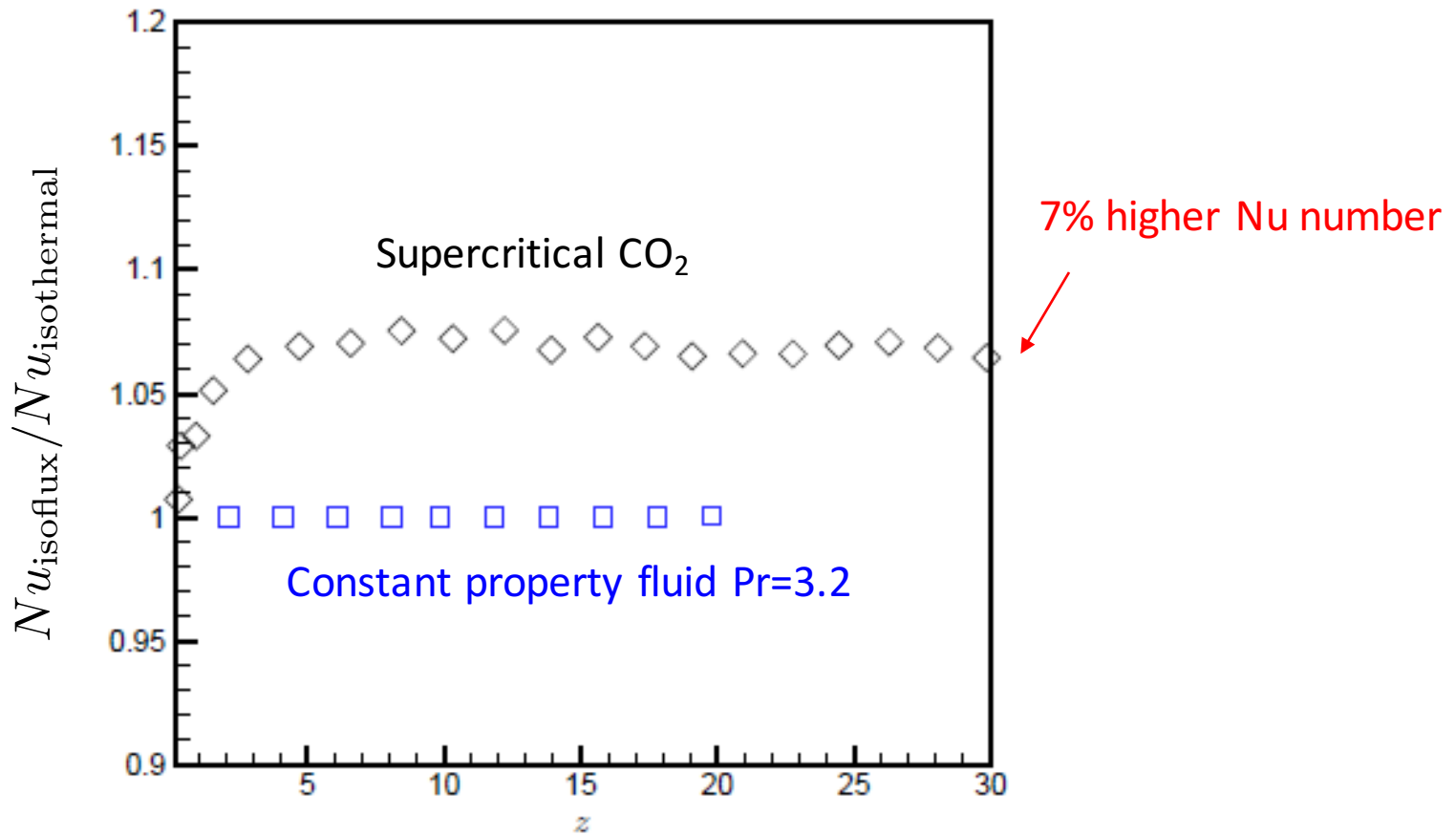
Additional heat flux  
caused by:

$$\alpha' \frac{\partial h'}{\partial r}$$

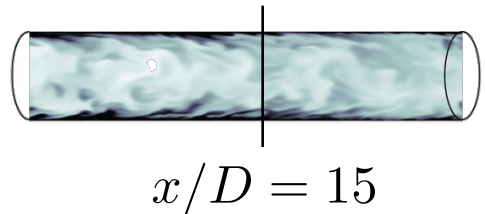


# Nusselt number ratio

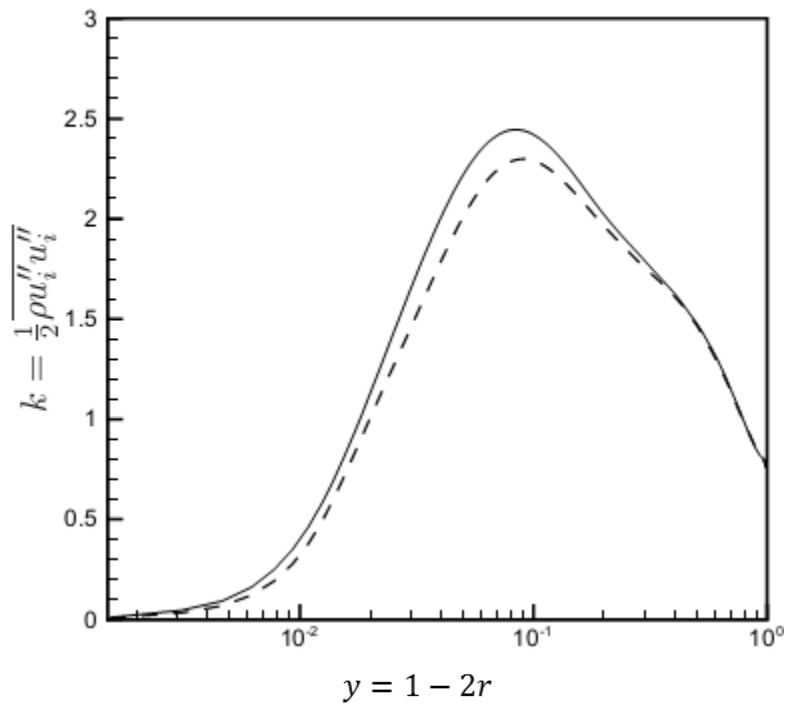
Nusselt number:  $Nu = \frac{\overline{\alpha \frac{\partial h}{\partial r}}|_w}{\lambda_b(T_w - T_b)}$



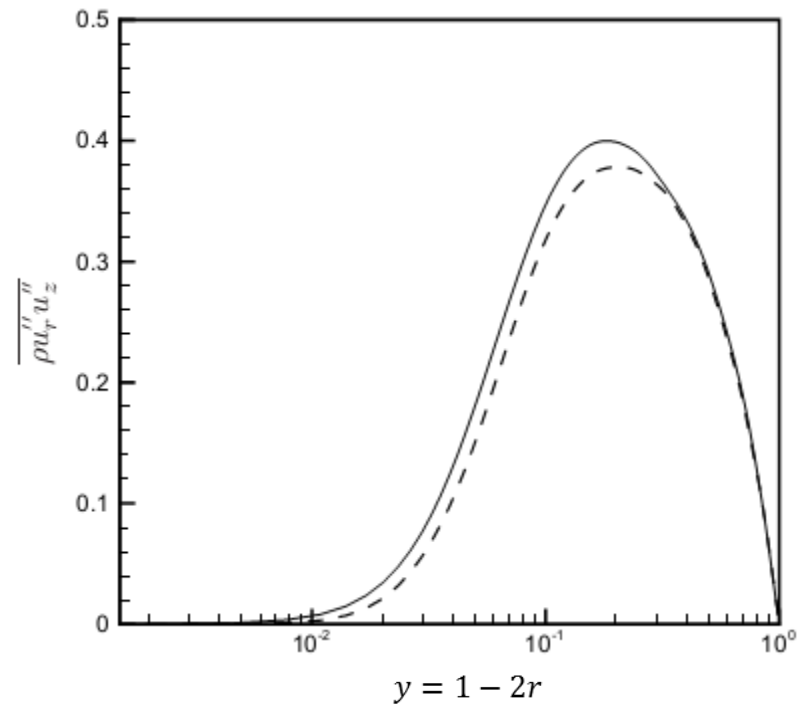
# Turbulent kinetic energy and Reynold shear stress



Turbulent kinetic energy



Reynolds shear stress



—  $K = \infty$   
- - -  $K = 0$

# Decomposed skin friction, FIK identity

(Fukagata, Iwamoto, Kasagi; PoF 2002)

$$C_{f,FIK} = -\frac{2}{\rho_b U_b^2 Re_{\tau 0}} \int_0^R r \bar{\mu} \bar{S}_{rz} r dr + \frac{2}{\rho_b U_b^2} \int_0^R r \bar{\rho} \bar{u}_r'' \bar{u}_z'' r dr - \left[ \frac{1}{\rho_b U_b^2} \int_0^R (R^2 - r^2) \frac{\partial \widetilde{p}}{\partial z} r dr + \frac{1}{\rho_b U_b^2} \int_0^R (R^2 - r^2) \frac{1}{r} \frac{\partial r \widetilde{\rho} \widetilde{u}_r \widetilde{u}_z}{\partial r} r dr \right. \\ + \frac{1}{\rho_b U_b^2} \int_0^R (R^2 - r^2) \frac{\partial \widetilde{\rho} \widetilde{u}_z \widetilde{u}_z}{\partial z} r dr + \frac{1}{\rho_b U_b^2} \int_0^R (R^2 - r^2) \frac{\partial \widetilde{\rho} \widetilde{u}_z'' \widetilde{u}_z''}{\partial z} r dr - \frac{1}{\rho_b U_b^2 Re_{\tau 0}} \int_0^R (R^2 - r^2) \frac{1}{r} \frac{\partial r \widetilde{\mu}' \widetilde{S}'_{rz}}{\partial r} r dr \\ \left. - \frac{1}{\rho_b U_b^2 Re_{\tau 0}} \int_0^R (R^2 - r^2) \frac{\partial \widetilde{\mu} \widetilde{S}_{zz}}{\partial z} r dr - \frac{1}{\rho_b U_b^2 Re_{\tau 0}} \int_0^R (R^2 - r^2) \frac{\partial \widetilde{\mu}' \widetilde{S}'_{zz}}{\partial z} r dr \right]$$

Where  $\widetilde{\Phi}(r, z) = \overline{\Phi}(r, z) - 8 \int_0^R \overline{\Phi}(r, z) r dr$

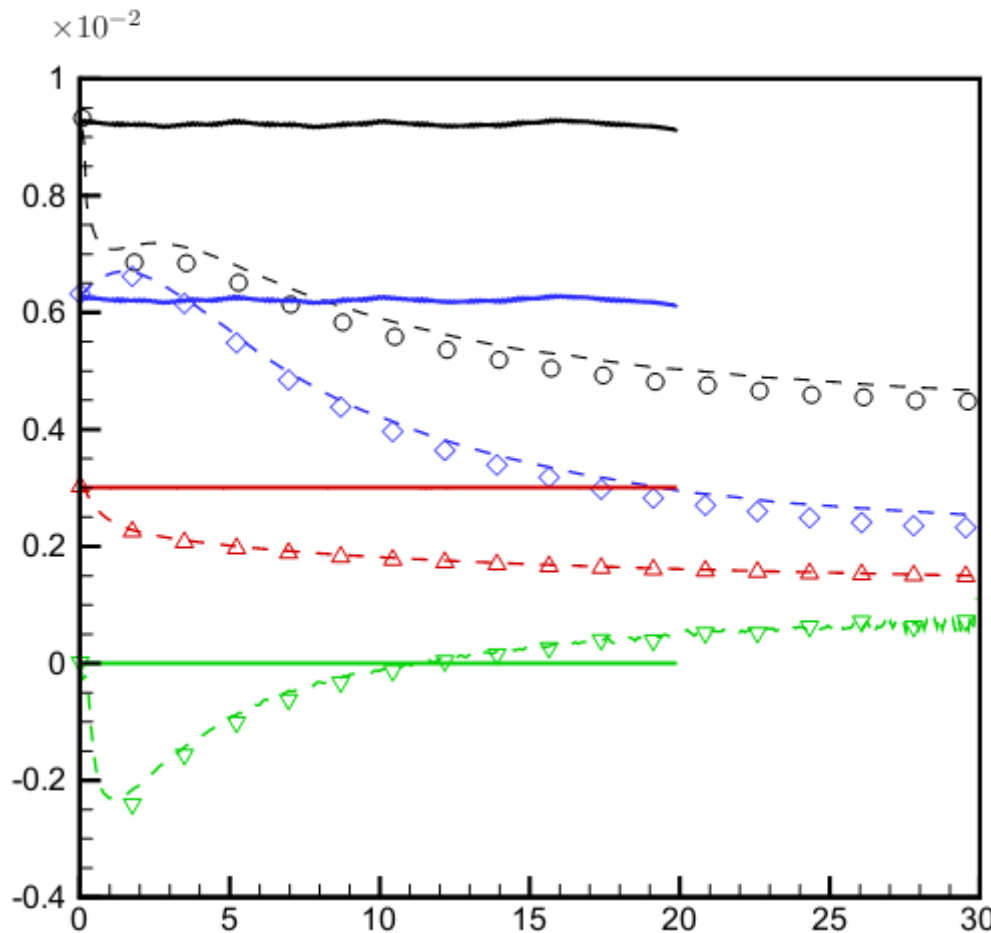
Laminar contribution Fully developed pipe flow with constant property fluid 

$$\frac{16}{Re_b}$$

Turbulent contribution

Inhomogeneous contribution

# Decomposed skin friction, FIK identity



Total skin friction

Laminar contribution

Turbulent contribution

Inhomogeneous contribution

Dashed lines: Iso-flux

Symbols: Iso-thermal

# Decomposed Nusselt number, FIK identity

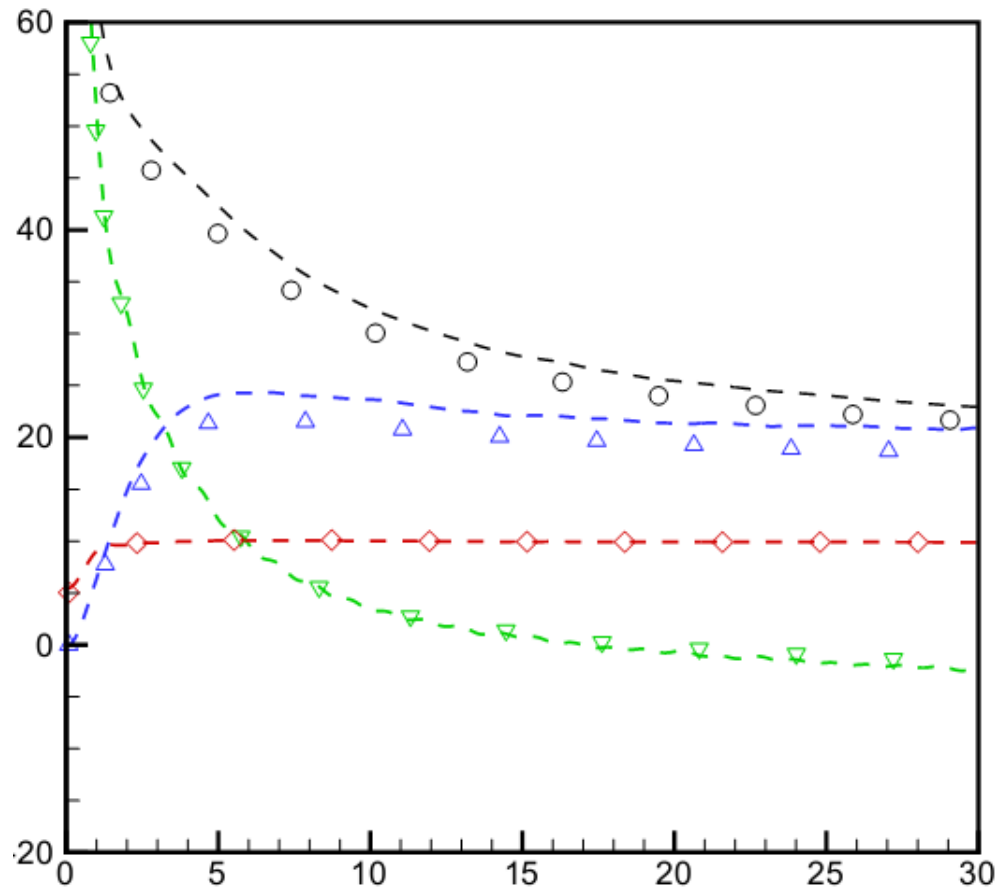
$$Nu_{FIK} = \boxed{\frac{32}{\lambda_b(T_w - T_b)} \int_0^R r \bar{\alpha} \frac{\partial \bar{h}}{\partial r} r dr} - \boxed{\frac{32 Re_{\tau 0} Pr_0}{\lambda_b(T_w - T_b)} \int_0^R r \bar{\rho} \bar{h}'' \bar{u}_r'' r dr} - \boxed{\frac{16 Re_{\tau 0} Pr_0}{\lambda_b(T_w - T_b)} \int_0^R (R^2 - r^2) \frac{1}{r} \widetilde{\frac{\partial r \bar{\rho} \tilde{h} \tilde{u}_r}{\partial r}} r dr} \\ - \boxed{\frac{16 Re_{\tau 0} Pr_0}{\lambda_b(T_w - T_b)} \int_0^R (R^2 - r^2) \widetilde{\frac{\partial \bar{\rho} \tilde{h} \tilde{u}_z}{\partial z}} r dr} - \boxed{\frac{16 Re_{\tau 0} Pr_0}{\lambda_b(T_w - T_b)} \int_0^R (R^2 - r^2) \widetilde{\frac{\partial \bar{\rho} \bar{h}'' \bar{u}_z''}{\partial z}} r dr} + \boxed{\frac{16}{\lambda_b(T_w - T_b)} \int_0^R (R^2 - r^2) \frac{1}{r} \widetilde{\frac{\partial r}{\partial r}} \widetilde{\frac{\alpha' \partial h'}{\partial r}} r dr} \\ + \boxed{\frac{16}{\lambda_b(T_w - T_b)} \int_0^R (R^2 - r^2) \widetilde{\frac{\partial}{\partial z}} (\bar{\alpha} \widetilde{\frac{\partial \bar{h}}{\partial z}}) r dr} + \boxed{\frac{16}{\lambda_b(T_w - T_b)} \int_0^R (R^2 - r^2) \widetilde{\frac{\partial}{\partial z}} (\alpha' \widetilde{\frac{\partial h'}{\partial z}}) r dr}$$

Laminar contribution

Turbulent contribution

Inhomogeneous contribution

# Decomposed Nusselt number, FIK identity



Total Nusselt number

Laminar contribution

Turbulent contribution

Inhomogeneous contribution

Dashed lines: Iso-flux

Symbols: Iso-thermal

# Conclusions

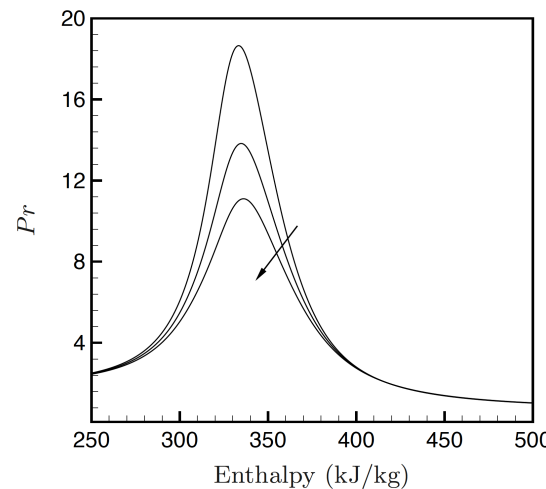
- Thermal effusivity ratio has an effect on heat transfer even for  $\text{Pr} > 1$  in supercritical flows
- Nusselt number 7% higher for  $K = \infty$
- The turbulent heat flux and Reynolds shear stress decrease
- Higher enthalpy fluctuations for  $K = \infty$  induce higher density fluctuations, which result in larger velocity fluctuations and thus higher mixing

# Thermal activity ratio and Prandtl number examples

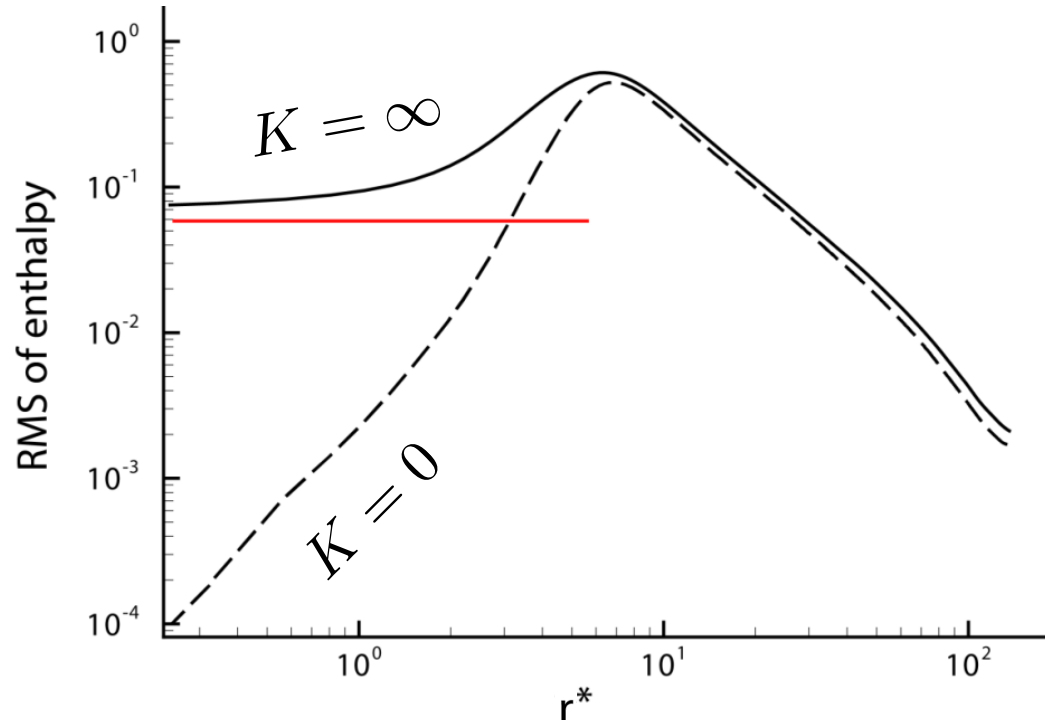
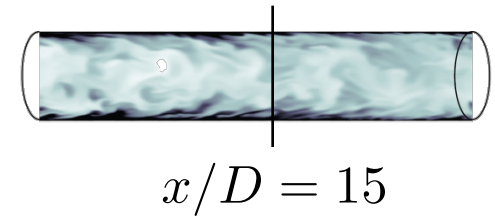
Prandtl number	Air * 0.708	Water * 6.78	scCO <sub>2</sub> ~ 4 - 16
Aluminum	0.00025	0.071	
Nickel based alloy	0.00073	0.207	~0.3
Copper	0.00015	0.044	
Glass	0.00419	1.190	
Plexiglas	0.00942	2.680	

\* based on Kasagi et al., Journal of heat transfer, 1989

Prandtl number for CO<sub>2</sub> at 80 bar



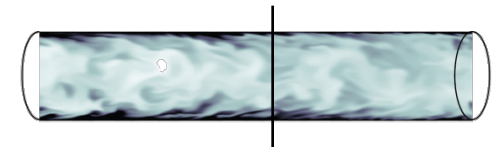
# Temperature rms values for constant properties



Reynolds decomposition of wall heat flux:

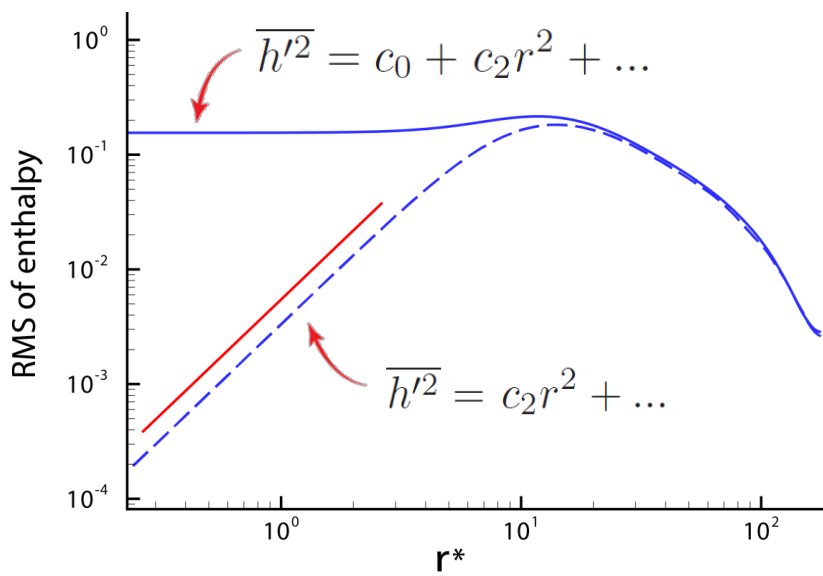
$$Q_w = \bar{\alpha} \frac{\partial \bar{h}}{\partial r}|_w + \alpha' \frac{\partial h}{\partial r}|_w + \bar{\alpha} \frac{\partial h'}{\partial r}|_w \rightarrow \frac{\partial \bar{h}'}{\partial r} = -\frac{2}{\bar{\alpha}} \bar{h}' \alpha' \frac{\partial h}{\partial r}$$

# Temperature rms values for constant properties



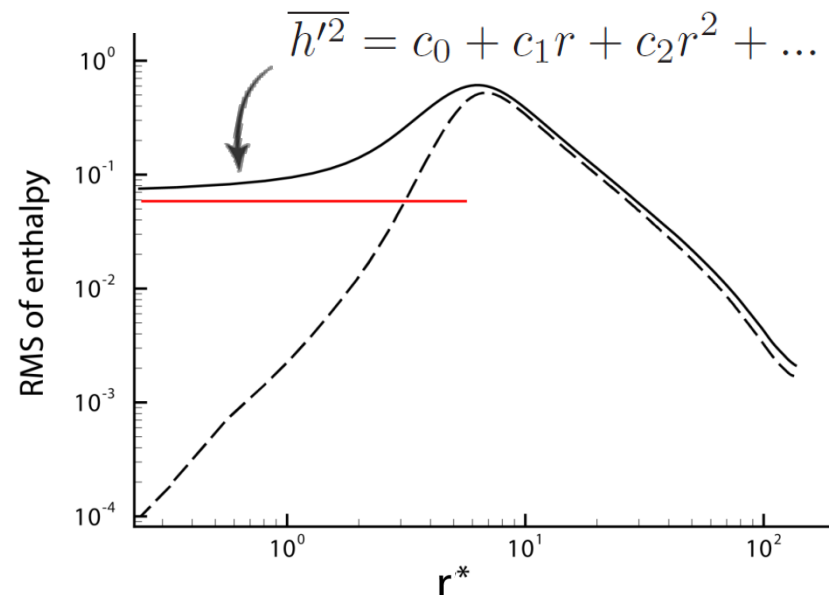
Constant property flow ( $\text{Pr}=3.2$ )

$$\frac{\partial \overline{h'^2}}{\partial r} = 0$$



Supercritical fluid flow ( $\text{Pr}_0=3.2$ )

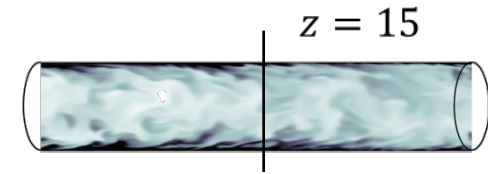
$$\frac{\partial \overline{h'^2}}{\partial r} = -\frac{2}{\alpha} \overline{h' \alpha'} \frac{\partial h}{\partial r}$$



# Radial heat fluxes

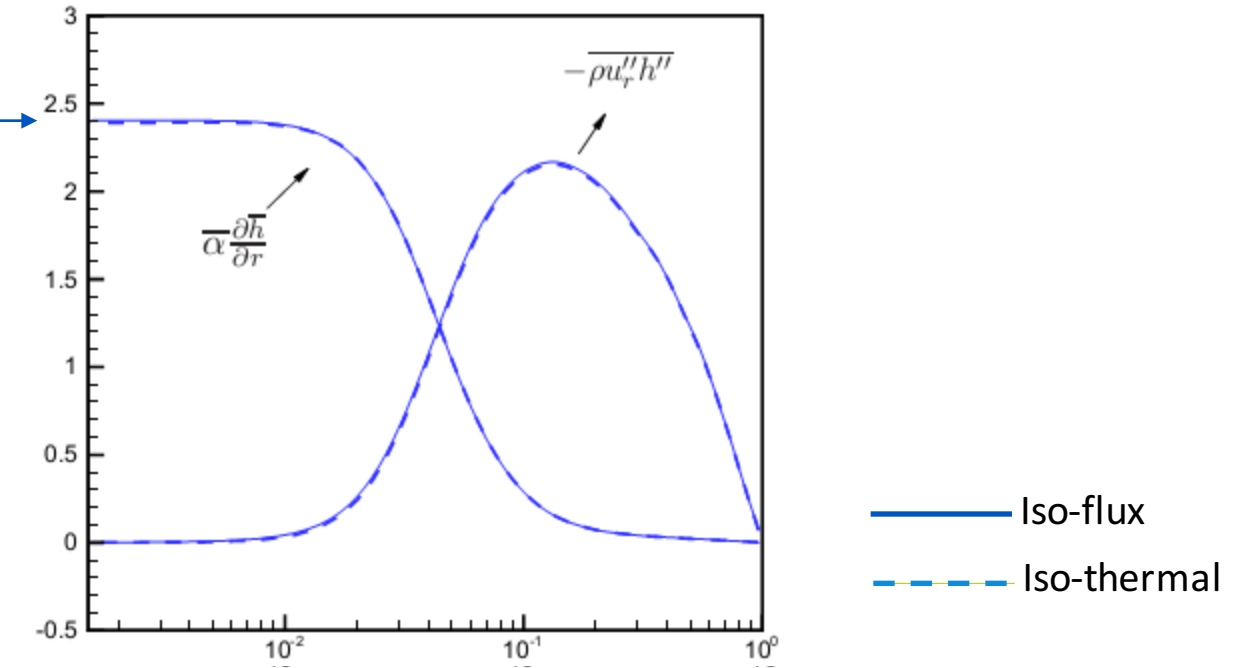
Total radial heat flux:

$$q_{r,tot} = \bar{\alpha} \frac{\partial \bar{h}}{\partial r} + \bar{\alpha}' \frac{\partial h'}{\partial r} - \bar{\rho} u_r'' h''$$

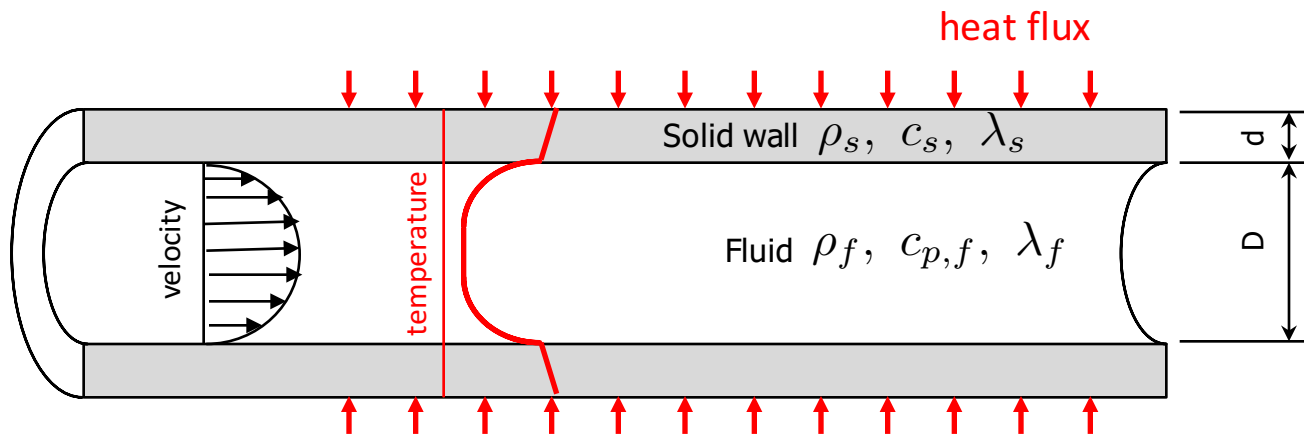


## Constant property (CP) flow

Specified heat  
flux = 2.4



# Effect of wall thickness on temperature fluctuations



Dimensionless wall thickness:

$$y^{++} = \sqrt{\lambda_f / \lambda_s} y^+$$

